



Kinetic, Equilibrium and Thermodynamic Studies of the Adsorption of Methylene Blue from Synthetic Wastewater Using Cow Hooves

Ilesanmi Osasona^{1*}, Oluwabamise Lekan Faboya¹
and Anthony Olawale Oso¹

¹Department of Chemical Sciences, Afe Babalola University, P.M.B. 5454, Ado-Ekiti, Nigeria.

Authors' contributions

This work was carried out in collaboration between authors. Author IO designed the study, performed the statistical analysis, wrote the protocol, and wrote the first draft of the manuscript. Authors IO and AOO managed the analyses of the study. Author OLF managed the literature searches. All authors read and approved the final manuscript.

Research Article

Received 13th March 2013
Accepted 4th June 2013
Published 12th July 2013

ABSTRACT

Aims: To investigate the feasibility and the kinetic of using cow hooves (CH) as a low-cost adsorbent for the removal of methylene blue (MB) from synthetic wastewater.

Place and Duration of Study: Chemistry Laboratory, Afe Babalola University, Ado-Ekiti, Nigeria, from October 2012 to January 2013.

Methodology: This study was conducted through batch process. The influence of initial pH, contact time, CH dosage and temperature on the adsorption property of CH was investigated using pH ranging from 2.0–11.0, contact time of 5–180 minutes, CH dosage of 0.15–1.0 g and temperature of 298–318 K. All experiments were carried out using 0.25 g of CH per 100 mL of MB solution except for effect of CH dosage. The equilibrium studies were carried out using MB concentration ranging from 10–100 mgL⁻¹ at 298, 308 and 318 K and the experimental data obtained were analysed and modelled using Langmuir, Freundlich, Dubinin-Radushkevich (D-R) and Temkin isotherm models.

Results: Our results indicated that a time of 90 minutes was required for equilibrium to be attained for 25 mgL⁻¹ MB. The percentage removal of MB was found to increase with increase in pH. The isotherm data were best fitted by Temkin isotherm model. The kinetics modelling of the experimental data agreed with the pseudo-second-order model

*Corresponding author: E-mail: osasona@yahoo.com;

suggesting that chemisorption was the rate determining step. The values of the thermodynamic parameters (ΔG^0 , ΔH^0 and ΔS^0) revealed that the adsorption process was spontaneous at very low temperature, feasible and exothermic.

Conclusion: Cow hoof could be a promising low-cost adsorbent for the removal of methylene blue from wastewater and this could be best achieved at high MB pH and within a period of one and half hours.

Keywords: Adsorption isotherm; cow hooves; methylene blue; wastewater.

1. INTRODUCTION

A pure sample of water is said to be colourless. The moment water is coloured its purity and suitability to sustain healthy life becomes doubtful. Colours can be imparted to water bodies through oil spillage, untreated wastewater from chemical, paint, dye producing industries, etc. Dyes are used extensively in many industries such as textiles, paper, rubber, plastics, cosmetics and food, to colour their products [1]. These dyes are left in the industrial wastes and consequently discharged into the water bodies. The presence of very small amounts of dyes in water (less than 1 ppm for some dyes) is highly visible and undesirable [2]. It has been pointed out that over 100,000 commercial dyes with a rough estimated annual production rate of $7 \times 10^5 - 1 \times 10^6$ tonnes exist in the world [3] and 10–20% of the dyes are lost during manufacturing and dyeing processes [3]. This implies that great amount of dyes is released into the environment annually.

The presence of dyes in the aquatic environment is of great concern because of their adverse effects on human's health and the imbalance created on the ecosystem [4]. Many of these dyes have mutagenic, carcinogenic and teratogenic effects either when inhaled or when they come in contact with the skin [5,6]. Also, photosynthetic activity and growth of bacteria are hampered as a result of coloured effluents acquired by water bodies [7-9]. Therefore, the need to remove dyes from wastewater before they are emptied into the environment becomes extremely important.

The conventional methods employed for dye removal from industrial effluents include: precipitation, oxidation, membrane processes, coagulation and flotation and ion exchange [9]. But most of these methods are associated with inherent limitations such as high running cost, generation of secondary waste, incomplete/ inefficient dye removal. Adsorption has proved to be an effective and attractive process for the removal of non-biodegradable pollutants (including dyes) from wastewater [9,10]. Most commercial systems use activated carbon as adsorbent to remove dyes from wastewater because of its excellent adsorption ability. But its widespread use is limited due to high costs of manufacturing and regeneration. Many low cost adsorbents, including natural materials, biosorbents, and waste materials from industry and agriculture, have been proposed by several authors [11].

MB is a thiazine (cationic) dye, which is most commonly used for colouring paper, dyeing cottons and wools, etc. Several reports have been published on the use of low-cost biomaterials for the removal of methylene blue from aqueous solution. These include rejected tea [12], rice husk [13], spent cotton seed husk [14], *Streptomyces rimosus* [15], chaff [16] sewage sludges [17], rose wood sawdust [18] and *Spirodela polyrrhiza* [19]. Most of these biomaterials earlier published on biosorption of MB are of plant origin. This is one of the reasons that necessitated the use of cow hooves in this study. Besides this, CH (this will be used to represent cow hoof in the remaining parts of this paper) is made up of insoluble

protein called keratin [20] which contains some functional groups such as amino and carboxyl, which may likely enhance adsorption processes.

Piles of cow hooves, horns and bones have become an eyesore in Nigerian abattoirs. Many a times, the environment is rid of these non-biodegradable cow by-products by burning. But burning itself generates gases which contribute to greenhouse effect. Therefore, it is necessary to find a way of turning this inedible animal by-product into a useful material. Though report has it that keratin extracted from cow hooves has been exploited in making a special fire extinguishing foam used by airport fire and rescue teams across the UK [21]. The present study was conducted to investigate the possibility of utilizing powdered cow hooves as adsorbent for the removal of MB from aqueous solution as another way of putting cow hooves into a significant use.

2. MATERIALS AND METHODS

2.1 Adsorbent and Methylene Blue (MB) Solution

Cow hooves were obtained from an abattoir along Ekiti State University Road, Ado-Ekiti, Nigeria. The hooves were thoroughly washed with distilled water and sun dried for a month. After drying, the hooves were washed again with distilled water, dried in an oven, ground and sieved using sieve of mesh size 425 μm .

A stock solution containing 1000 mg/L of MB was prepared by dissolving 1.0 g of analytical grade MB in distilled water. Standard solutions of different concentrations as might be required were prepared (by dilution) from this stock solution.

2.2 Adsorption Studies

Adsorption experiments were carried out by batch process. A mixture containing 0.25 g of cow hoof powder and 100 mL MB solution of known concentration was equilibrated at 120 rpm using a thermostatic water bath shaker. The mixture was centrifuged after reaching the established agitation time and the concentration of MB present in the liquid phase (supernatant) was determined spectrophotometrically using UV/VIS spectrophotometer model 752 (Gallenkomp, UK). The absorbance of the colour was measured at 661nm where the maximum absorption peak exists. Calibration curve of absorbance versus concentration of the dye solution was plotted. The amount of MB adsorbed per unit mass of adsorbent was determined using the following equation:

$$q_e = \frac{(C_0 - C_f)V}{m} \quad (1)$$

Where, m is the mass of adsorbent (g), V is the volume of the solution (L), C_0 is the initial MB concentration (mgL^{-1}), C_f is the final MB concentration in the liquid phase (mgL^{-1}) and q is the amount of MB (mgg^{-1}) adsorbed. The percentage MB removal (%R), was calculated using the following expression:

$$\%R = \frac{(C_o - C_f) \times 100}{C_o} \quad (2)$$

2.3 Experimental Conditions

The effect of pH on the adsorption of MB was studied by contacting 100 mL solution of 25 mgL⁻¹ MB dye with 0.25g of CH at 298 K. The pH of MB was adjusted between pH 2.0 and pH 11.0 using 0.1 M NaOH or 0.1 M HCl. Digital Hanna instrument pH metre (HI 2210) was used for pH measurement. The pH of maximum adsorption was used for other experiments. The effect of contact time on the adsorption process was conducted at different agitation times ranging from 5-180 minutes using 100 mL of 25 mgL⁻¹ MB solution and 0.25 g CH at 298 K. Experiments to determine the effect of adsorbent mass were carried out using 100 mL of 25 mgL⁻¹ MB solution. The adsorbent mass was varied from 0.15-1.0 g and the flasks were agitated for 90 minutes. After equilibration, the final concentration of MB was determined and the percentage of MB adsorbed was calculated.

2.4 Equilibrium Studies

Equilibrium studies were conducted by contacting fixed amount of CH (0.25 g) with 100 mL of MB solution having concentrations ranging from 10-100 mgL⁻¹ at pH of 11 and temperature of 298, 308 and 318 K. The samples were then centrifuged and analysed as described earlier.

2.5 FTIR Characterization of CH

Infrared analysis was conducted on the CH to investigate the functional groups present on its surface in the range of 400-4000 cm⁻¹ using Fourier Transform Infra-Red spectrometer (Perkin-Elmer Spectrum GX, Beaconsfield, UK).

3. RESULTS AND DISCUSSION

3.1 FTIR Spectra of CH Surface

The FTIR spectra of CH were taken before and after the adsorption of MB to ascertain the possible involvement of the functional groups on the surface of CH in the adsorption of MB. The broad band at 3314 cm⁻¹ can be attributed to -OH stretching vibration while the band at 2931.42 cm⁻¹ can be assigned to the -CH stretching vibrations. The peak at 3314cm⁻¹ was strong and broad due to amine group stretching vibrations superimposed on the side of hydroxyl group band, which has been reported to occur at 3500-3300 cm⁻¹[22, 23]. The peaks at 1658.6 cm⁻¹, 1530.58 cm⁻¹ and 1393 cm⁻¹ may be attributed to C=O stretching, -NH bending and -CN vibrations of amides respectively [23]. The bands at 1239.11 cm⁻¹ and 1039.63 cm⁻¹ can be linked to C-O stretching [23]. Fig. 1 reveals that some new bands appeared, some remained and some were shifted after MB sorption. The bands at 3314, 1658.6, 1530.58, 1393, 1239.11 and 1039.63 cm⁻¹ were shifted to 3306, 1658.26, 1529, 1387.30, 1236.26, 1033.93 cm⁻¹ after MB adsorption. This is an indication that -OH, -C=O, -CO and -NH group could be involved in the adsorption of MB onto CH.

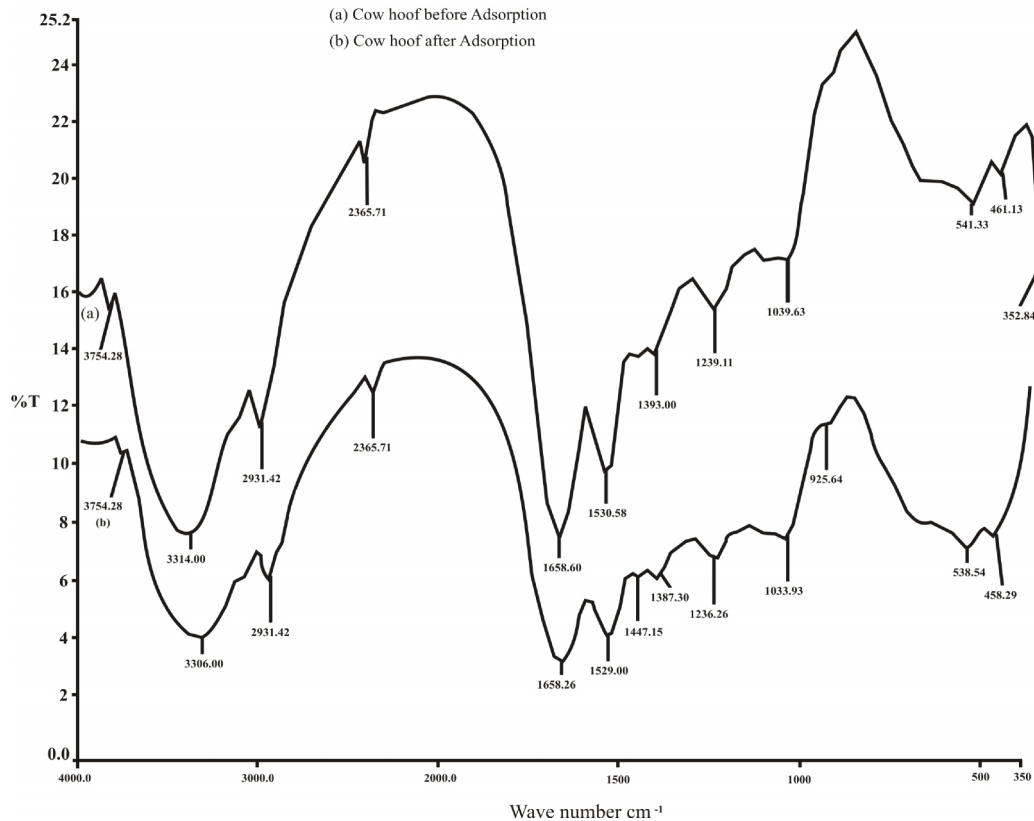


Fig. 1. FTIR spectra of CH (a) before adsorption and (b) after adsorption of MB

3.2 Effect of pH

The effect of solution pH on the adsorption of MB onto CH is depicted in Fig. 2. The figure reveals that pH variation had a significant influence on the adsorption process. The result shows that the adsorption of MB onto CH increases with increase in solution pH. It was observed that the percentage removal of MB increased from 38.05 to 95.67% when the pH was increased from 2 to 11. The influence of the solution pH on the dye uptake can be explained on the basis of the zero point charge or isoelectric point of the adsorbent [24]. The zero point charge (pH_{PZC}) of the cow hoof was determined to be 7.7 using the solid addition method [25]. It has been reported that adsorption of cations is favoured at $\text{pH} > \text{pH}_{\text{PZC}}$, while the adsorption of anions is favoured at $\text{pH} < \text{pH}_{\text{PZC}}$ [25]. This happens because at $\text{pH} > \text{pH}_{\text{PZC}}$, the surface of the adsorbent is negatively charged thereby supporting the uptake of more MB due to electrostatic force of attraction [24] between the negatively charged adsorbent surface and the positively charged MB. At lower pH ($\text{pH} < \text{pH}_{\text{PZC}}$), H^+ ions compete effectively with the cationic dye for the active sites on the adsorbent surface, thereby bringing about decrease in the amount of MB adsorbed. In addition, at pH lower than the pH_{PZC} , the surface of the adsorbent becomes positively charged. Therefore, forces of repulsion, which discourage adsorption of MB, exist between the adsorbent surface and the cationic dye at this stage. The adsorption of MB seemed to be uniform between pH 6 and 8. This observation could be linked to the fact that the pH_{PZC} (7.7) falls within this region; the

surface of the adsorbent has a charge of zero thereby bringing about little or no increase in the percentage of MB adsorbed at this region (pH 6 to 8). The percentage removal of MB slightly picked up at pH higher than this region (Fig. 2).

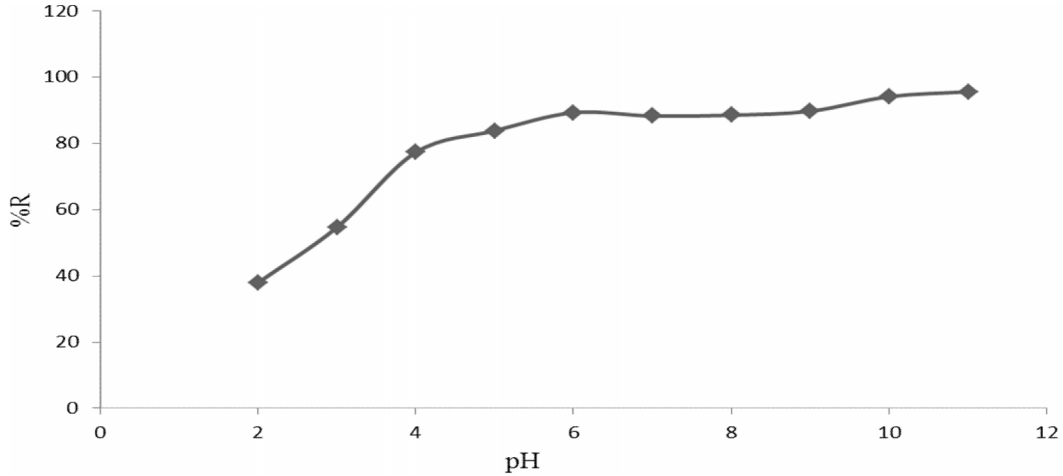


Fig. 2. Effect of pH on the adsorption of MB onto CH ($C_o = 25 \text{ mgL}^{-1}$, volume of MB = 100 mL, mass of CH = 0.25 g, temperature= 298 K)

3.2 Effect of Contact Time

Contact time is an important factor that affects uptake efficiency in batch adsorption processes. Fig. 3 reveals that the maximum adsorption of MB occurred after 90 minutes of equilibration with percentage removal of 83.42%. The rate of the adsorption process increased rapidly in the first 30 minutes and then grew more slowly as the agitation time increased beyond 30 minutes. The rapid removal of MB at the initial stage may be attributed to (i) the rapid attachment of dye molecules to the surface of the adsorbent and also (ii) the increased number of binding sites available, consequently leading to an increase in driving force of the concentration gradient between adsorbate in solution and adsorbate-adsorbent interaction [26,27]. The rate of adsorption seemed to be insignificant when the agitation time was above 90 minutes. This implies that the adsorption process nearly reached equilibrium within the first 90 minutes of agitation. This observation is similar to literature reports on the adsorption of MB [26,27].

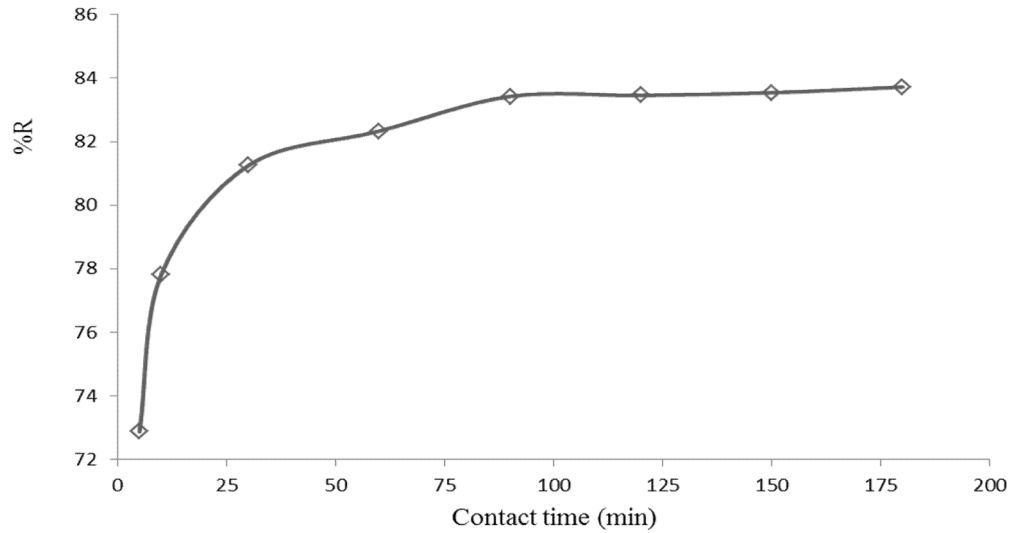


Fig. 3. Effect of contact time on the adsorption of MB onto CH ($C_o = 25 \text{ mgL}^{-1}$, volume of MB = 100 mL, mass of CH = 0.25 g, pH = 11, temperature = 298 K)

3.3 Effect of Sorbent Mass

The effect of adsorbent mass on the adsorption study is shown in Fig. 4. The figure reveals that percentage MB removal (%R) is highly a function of the mass of the adsorbent used. The percentage of MB adsorbed increased with increase in the mass of the adsorbent dosed. This behaviour can be attributed to increased adsorbent surface area, which invariably increases the number of adsorption sites available for adsorption. The percentage removal of MB increased from 80.27 to 89.63% as the adsorbent mass was raised from 0.15 – 1.0 g. It can also be observed from the figure that the amount of MB adsorbed per gram of CH (q_e) decreased by 11.14 mgg^{-1} as the mass of adsorbent added increased from 0.15 – 1.0 g. The decrease in adsorption capacity (q_e) is basically due to the sites remaining unsaturated during the adsorption process [28]. Results similar to this have been reported by several authors [11,14,28].

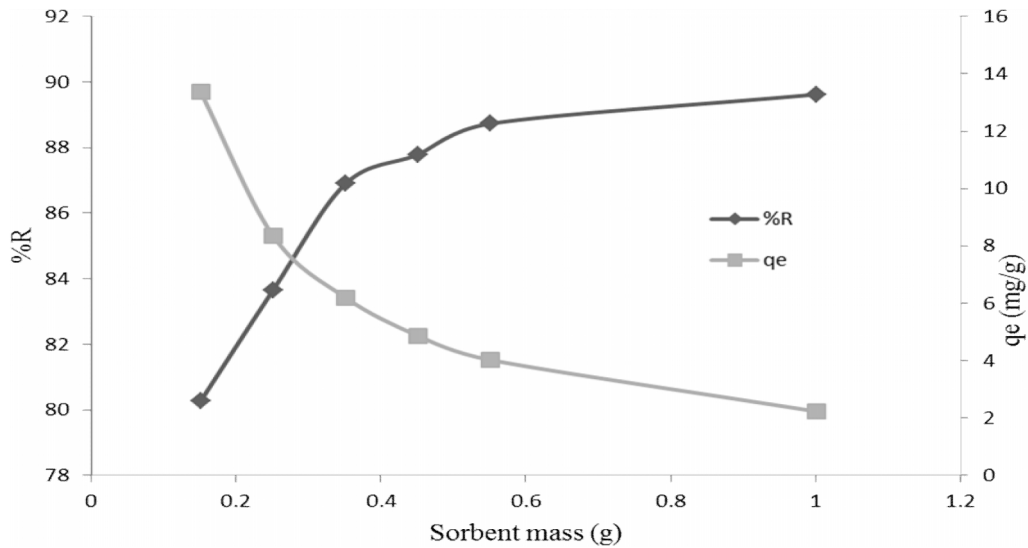


Fig. 4. Effect of sorbent mass on the adsorption of MB onto CH ($C_o = 25 \text{ mgL}^{-1}$, volume of MB = 100 mL, contact time = 90 minutes, pH = 11, temperature = 298 K)

3.4 Effect of Initial MB Concentration and Temperature

The effect of temperature on the adsorption of MB onto CH was investigated at 298, 308, and 318 K using initial MB concentration of 10–100 mgL^{-1} (Fig. 5). As shown by Fig. 5, the equilibrium uptake of MB increased with increase in the initial MB concentrations for all temperatures. For example, when the initial MB concentration was increased from 10 to 100 mgL^{-1} , the uptake capacity of CH increased from 3.32–31.02, 3.31–30.59 and 3.3–30.08 mgg^{-1} at 298 K, 308 K and 318 K respectively. This occurs because higher initial concentration provides an important driving force to overcome all mass transfer resistances of the MB between the aqueous and solid phases [16,29]. Similar results on the influence of initial MB concentration on equilibrium adsorption capacity have been reported [17,29]. It can be observed from the figure that the equilibrium uptake of MB adsorption decreased steadily when the temperature was increased from 298 to 318 K. This suggests that the adsorption of MB onto CH is an exothermic process and the mechanism is mainly physical adsorption [17].

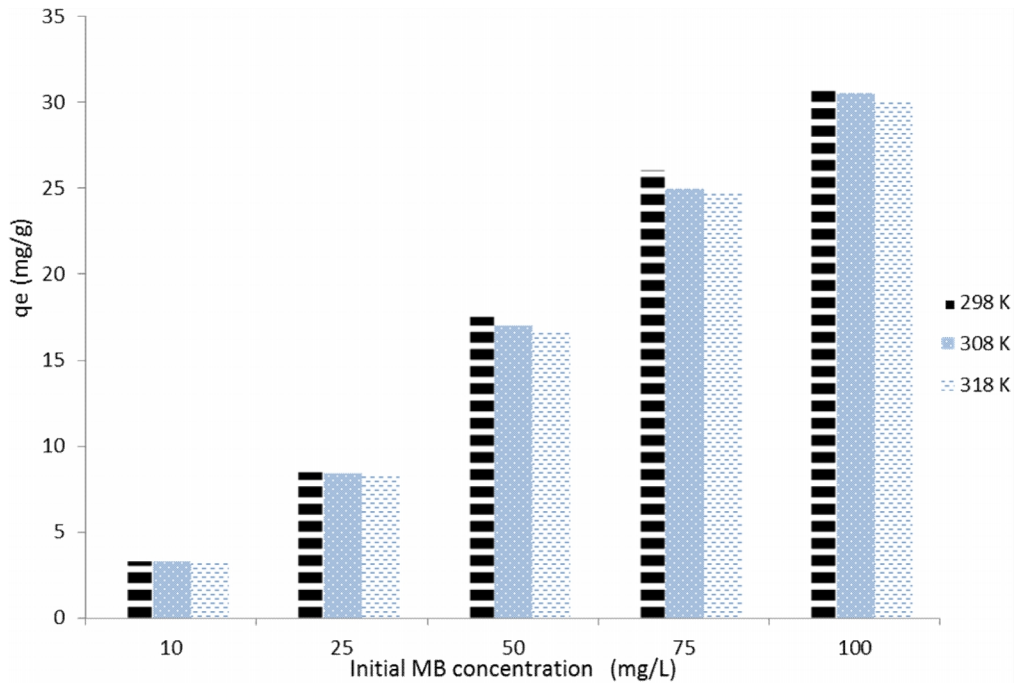


Fig. 5. Effect of temperature and initial MB concentration on the removal of MB by CH (volume of MB = 100 mL, contact time = 90 minutes, pH = 11, mass of CH = 0.25 g)

3.5 Adsorption Isotherms

Many adsorption isotherm models are used to describe equilibrium data but in this study, Langmuir, Freundlich, Dubinin-Radushkevich (D-R) and Temkin models were chosen to describe the relationship between the amount of MB adsorbed on CH and its equilibrium concentration at three different temperatures. The correlation coefficient R^2 value of each plot was used to describe the applicability of the isotherm models.

Langmuir model assumes a monolayer adsorption of adsorbates on a homogeneous surface without any interaction between the adsorbed molecules. The model takes the following linear form [30]:

$$\frac{C_e}{q_e} = \frac{1}{K_L q_m} + \frac{C_e}{q_m} \quad (3)$$

Where, q_m (mg g^{-1}) is the maximum adsorption capacity, K_L (L mg^{-1}) is a constant related to the affinity of binding sites or bonding energy. The values of q_m and K_L can be estimated from the slope and intercept of the linear plot of C_e/q_e versus C_e respectively.

The Freundlich isotherm model is based on adsorption on a heterogeneous surface. It can be expressed linearly as [31]:

$$\log q_e = \log K_f + \frac{1}{n} \log C_e \quad (4)$$

where K_f and n are Freundlich constants which are related to adsorption capacity and intensity respectively. The values of K_f and $1/n$ can be obtained from the slope and intercept of the linear plot of $\log q_e$ against $\log C_e$.

The derivation of the Temkin isotherm assumes that the heat of adsorption of all molecules decreases linearly when the layer is covered and that the adsorption has a maximum energy distribution of a uniform bond. The linearized form of Temkin equation can be expressed as [32]:

$$q_e = B \ln K_T + B \ln C_e \quad (5)$$

Where $B=RT/b_T$, K_T (Lmol^{-1}) is the equilibrium binding constant corresponding to the maximum binding energy, R is the universal gas constant ($8.314 \text{ Jmol}^{-1}\text{K}^{-1}$), T is the absolute temperature in Kelvin and b_T (Jmol^{-1}) is a constant that describes the nature of the adsorption energy. A positive value of b_T indicates that the adsorption process is exothermic while a negative value of b_T is an indication of endothermic process [26]. The values of b_T and K_T can be obtained from the slope and intercept of the linear plot of q_e versus $\ln C_e$ respectively.

The linear form of Dubinin–Radushkevich (D–R) isotherm can be expressed as follows [33]:

$$\ln q_e = \ln q_D - \beta \varepsilon^2 \quad (6)$$

Where ε is the Polanyi potential = $RT \ln(1 + 1/C_e)$, q_D is the adsorption capacity of the adsorbent (mgg^{-1}), β is a constant related to the adsorption energy ($\text{mol}^2 \text{ kJ}^{-2}$), R is the gas constant ($\text{kJK}^{-1} \text{ mol}^{-1}$), and T is the temperature (K). The D-R model is important for predicting the nature of adsorption process through the determination of the mean adsorption energy (E) using equation (7)

$$E = (-2\beta)^{-1/2} \quad (7)$$

If $E < 8 \text{ kJmol}^{-1}$, the adsorption is dominated by physisorption, if E is between 8 and 16 kJmol^{-1} , the adsorption process is dominated by chemisorption mechanism and if $E > 16 \text{ kJmol}^{-1}$, the adsorption process is dominated by particle diffusion [34].

The different isotherm parameters with their correlation coefficient values are presented in Table 1. It can be seen from the correlation coefficient values that the Temkin isotherm model fitted the data best followed by the Freundlich model. The positive values of the Temkin constant b_T at all temperatures further confirms that the adsorption process is exothermic in nature while the values obtained for the Freundlich constant n ($1 < n < 10$) is an indication that CH has a high affinity for MB molecules. The mean adsorption energy E calculated from D-R model reveals that the adsorption of MB onto CH was dominated by physical adsorption since all values of E are less than 8 kJmol^{-1} . The maximum adsorption capacity q_m (Langmuir), K_f (Freundlich) and q_D (D-R) showed a slight decrease in value as the temperature increased from 298 – 318 K.

Table 2 is a comparison between the Langmuir maximum adsorption capacity q_m for this study and the q_m of some earlier literature reports on low-cost adsorbents. A direct comparison of different low-cost adsorbents might be difficult due to varying experimental conditions employed in the studies [35], yet CH shows a high adsorption capacity when compared with other low-cost adsorbents that have been investigated for the removal of MB from aqueous solutions.

Table 1. Isotherm parameters for the removal of MB by CH

| Isotherm | Parameter | Temperature (K) | | |
|------------|---|-----------------|--------|--------|
| | | 298 | 308 | 318 |
| Langmuir | q_m (mgg ⁻¹) | 77.52 | 76.34 | 76.34 |
| | K_L (Lmg ⁻¹) | 0.0349 | 0.0322 | 0.0294 |
| | R^2 | 0.5096 | 0.7053 | 0.7654 |
| Freundlich | K_f (mgg ⁻¹)(Lmg ⁻¹) ^{1/n} | 2.56 | 2.4 | 2.26 |
| | n | 1.107 | 1.085 | 1.149 |
| | R^2 | 0.9133 | 0.9611 | 0.9696 |
| D-R | q_D (mgg ⁻¹) | 23.91 | 22.71 | 21.4 |
| | E (kJmol ⁻¹) | 0.558 | 0.56 | 0.564 |
| | R^2 | 0.8875 | 0.8875 | 0.8517 |
| Temkin | B | 11.66 | 11.014 | 10.687 |
| | K_T (Lmol ⁻¹) | 0.7158 | 1.463 | 0.65 |
| | b_T (Jmol ⁻¹) | 212.3 | 232.49 | 247.39 |
| | R^2 | 0.9567 | 0.981 | 0.9661 |

Table 2. Comparison of maximum monolayer capacity (q_m) of MB adsorbed by various low-cost adsorbents

| Adsorbent | q_m (mgg ⁻¹) | Reference |
|---|----------------------------|---------------|
| Peanut hull treated with sulphuric acid | 147 | [7] |
| Phoenix leaves | 80.9 | [11] |
| Spent cottonseed husk | 143.5 | [14] |
| Natural chaff | 20.3 | [16] |
| Giant duck weed | 129.87 | [19] |
| Rice straw | 32.6 | [26] |
| Alkali treated rice straw | 62.9 | [26] |
| Rice husk | 40.6 | [36] |
| Dead <i>Aspergillus niger</i> | 18.54 | [37] |
| Yellow passion fruit waste | 44.7 | [38] |
| Cow hoof | 77.52 | Current study |

3.6 Adsorption Kinetics

The pseudo-first-order, pseudo-second order and intra-particle diffusion models were used to evaluate the kinetic parameters for the adsorption process. The pseudo-first-order equation can be expressed as [39, 40]:

$$\log(q_e - qt) = \log q_e - \frac{k_1 t}{2.303} \tag{8}$$

Where k_1 = the rate constant for pseudo-first-order equation (min^{-1}) and q_e = amount of dye adsorbed at equilibrium (mgg^{-1}). A plot of $\log (q_e - q_t)$ against t gave a straight line. The values of q_e and k_1 (Table 3) were computed from the slope and intercept of the plot.

The linear form of the pseudo-second model can be expressed as [39,40]:

$$\frac{t}{q_t} = \frac{1}{k_2 q_e^2} + \frac{1}{q_e} t \tag{9}$$

where k_2 is the pseudo-second-order adsorption rate constant ($\text{gmg}^{-1} \text{min}^{-1}$). The values of q_e and k_2 can be evaluated from the slope and intercept of the plot of t/q_t against t respectively.

Intra-particle diffusion mechanism was also studied to investigate the diffusion mechanism of the adsorption of MB onto CH. The linear expression for intra-particle diffusion model is given by equation 10 [41].

$$q_t = k_{di} t^{0.5} + C_i \tag{10}$$

where k_{di} ($\text{mg/g min}^{1/2}$), $t^{0.5}$ ($\text{min}^{1/2}$) and C_i are the intra-particle diffusion rate constant, square root of time, and intercept at stage i , respectively. Values of k_{di} and C_i can be calculated from the slope and intercept of linear portion of the plot of q_t against time. The value of C_i is related to the thickness of boundary layer.

Fig. 6 shows the diffusion plot of q_t against $t^{0.5}$ for MB adsorption onto CH at 298 K. If intra-particle diffusion occurs, then q_t versus $t^{0.5}$ will be linear and if the plot passes through the origin, then the rate-limiting process is only due to intra-particle diffusion. Otherwise, some other mechanism along with intra-particle diffusion is also involved [12]. The result presented in Fig. 6 clearly shows that the adsorption process seems to display two linear portions which are not linear over the whole time. The first stage (the first 60 minutes) is the instantaneous or external surface adsorption, that is, the diffusion of the adsorbate through the solution to the external surface of the absorbent [26]. The second stage (period above 60 minutes) is the phase of gradual adsorption where intra-particle diffusion is the rate-controlling step.

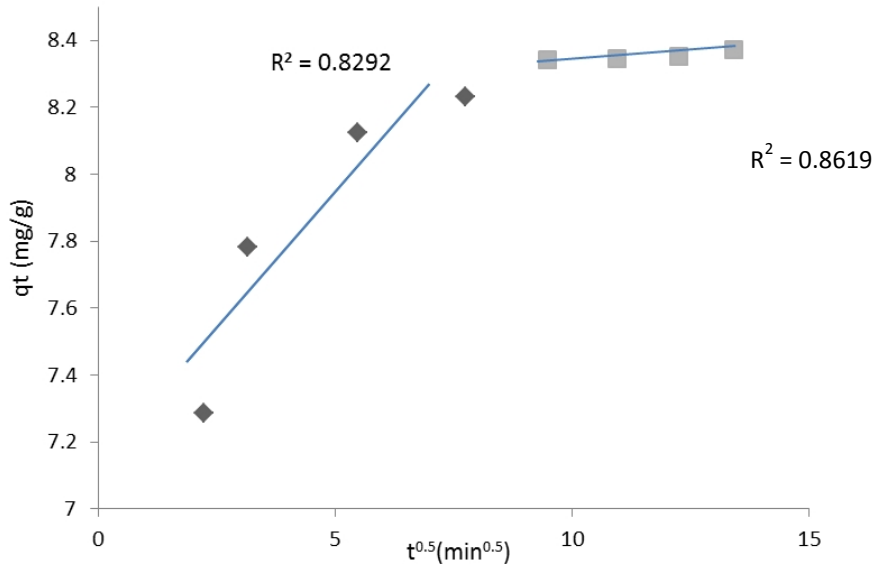


Fig. 6. Intra-particle diffusion plots for the adsorption of MB onto CH at 298 K

The $q_{e(\text{cal})}$ from pseudo-second-order kinetics model closely agrees with $q_{e(\text{exp})}$ value while the value from pseudo-first-order kinetics model does not. This implies that the adsorption mechanism of MB on CH is better described by pseudo-second-order kinetics. This is further confirmed by the correlation coefficient (R^2) for pseudo-second-order kinetics (Table 3). This observation suggests that chemisorption might be the rate-limiting step that controlled the adsorption of MB onto CH.

Table 3. Kinetics parameters for the adsorption of MB on CH at 298K

| Pseudo-first-order | | Pseudo-second-order | | | Intra-particle diffusion | | | |
|--|--|------------------------|--------|--|---------------------------------------|-------|--|--|
| $q_{e(\text{exp})}$ (mgg^{-1}) | $q_{e(\text{cal})}$ (mgg^{-1}) | $k_1(\text{min}^{-1})$ | R^2 | $q_{e(\text{cal})}$ (mgg^{-1}) | $k_2(\text{gmg}^{-1}\text{min}^{-1})$ | R^2 | $k_{d1}((\text{mgg}^{-1}\text{min}^{-0.5}))$ | $k_{d2}(\text{mgg}^{-1}\text{min}^{-0.5})$ |
| 8.32 | 0.949 | 0.0168 | 0.9229 | 8.41 | 0.128 | 1 | 0.16 | 0.07 |

3.7 Thermodynamic Parameters for the Adsorption of MB onto CH

Thermodynamic studies were done by carrying out equilibrium studies at different temperatures to determine the thermal effect of the process and assess its spontaneity. The changes in free energy (ΔG), enthalpy (ΔH) and entropy (ΔS) were determined using the following equations [34]:

$$\Delta G = -RT \ln K_L \tag{11}$$

$$\ln K_L = \Delta S/R - \Delta H/RT \tag{12}$$

where, R is the ideal gas constant ($\text{kJmol}^{-1}\text{K}^{-1}$), K_L is the Langmuir constant and T is the temperature in Kelvin. The values of ΔH and ΔS can be obtained from the slope and intercept of the linear plots of $\ln K_L$ against $1/T$.

The values for the thermodynamic parameters are shown in Table 4. The adsorption of MB on CH can be described as exothermic judging from the negative value of ΔH . The negative value of ΔS indicates that the adsorption of MB onto CH proceeds in the direction of decrease in entropy while the values of ΔG at various temperatures suggest that the adsorption process is feasible at very low temperatures

Table 4. Thermodynamic constants for the adsorption of MB on CH at different temperatures

| T (K) | ΔG (kJ mol ⁻¹) | ΔH (kJ mol ⁻¹) | ΔS (kJ mol ⁻¹) | R (kJ mol ⁻¹ K ⁻¹) |
|-------|------------------------------------|------------------------------------|------------------------------------|---|
| 298 | 8.302 | -6.817 | -0.0507 | 8.314 x 10 ⁻³ |
| 308 | 8.8076 | | | 8.314 x 10 ⁻³ |
| 318 | 9.315 | | | 8.314 x 10 ⁻³ |

4. CONCLUSION

The adsorption of MB from aqueous solution by CH was observed to be influenced by the solution pH, contact time, adsorbent dosage and initial MB concentration. The adsorption capacity of CH was found to increase with increase in pH and initial MB concentration. The equilibrium data fitted well with Temkin and Freundlich isotherm models. The Langmuir maximum adsorption capacity (q_m) show a slight decrease with increase in temperature. The Freundlich constant (n) revealed that the adsorption process was favourable while the mean adsorption energy (E) evaluated from Dubinin-Radushkevich showed that the adsorption of MB onto CH was dominated by physisorption. The kinetic modelling of adsorption of MB onto CH followed the pseudo-second-order kinetic model while the intra-particle diffusion model indicated that two steps were involved in the adsorption mechanism and that intra-particle diffusion with other mechanism were involved in the rate-controlling step. The thermodynamic studies showed that the adsorption process was feasible, spontaneous (at very low temperature) and exothermic.

COMPETING INTERESTS

There are no competing interests.

REFERENCES

1. Belala Z, Jeguirim M, Belhachemi M, Addoun F, Trouvé. Biosorption of basic dye from aqueous solutions by date stones and palm-trees waste: Kinetic, equilibrium and thermodynamic studies. *Desalination*. 2011;271:80–87.
2. Crini G. Non-Conventional low-cost adsorbents for dye removal: A review. *Bioresour Technol*. 2006;97:1061–1085.
3. Ghaedia M, Hajati S, Karimia F, Brazesha B, Ghezlbash G. *Saccharomyces cerevisiae* for the biosorption of basic dyes from binary component systems and the high order derivative spectrophotometric method for simultaneous analysis of brilliant green and methylene blue. *J Ind Chem and Eng*. 2010; Article in press
4. Inthorn D, Singhtho S, Thiravetyan P, Khan E. Decolourization of basic, direct and reactive dyes by pre-treated narrow-leaved cattail (*Typha angustifolia* Linn.), *Bioresour Technol*. 2004;94:299–306.

5. Sadhasivam S, Savitha S, Swaminathan K. Exploitation of trichoderma harzianum mycelial waste for the removal of rhodamine 6G from aqueous solution. J Environ Manage. 2007;85:55–161.
6. Maurya NS, Mittal AK, Cornel P, Rother E. Biosorption of dyes using dead macro fungi: Effect of dye structure, ionic strength and pH. Bioresour Technol. 2006;97:512–521.
7. Özer D, Dursun G, Özer A. Methylene blue adsorption from aqueous solution by dehydrated peanut hull. J Hazard Mater. 2007;144:171–179.
8. Suteu D, Bilba D, Aflori M, Doroftei F, Lisa G, Badeanu M, Malutan T. The seashell wastes as biosorbent for reactive dye removal from textile effluents. Clean – Soil, Air, Water. 2012;40(2):198–205.
9. Robinson T, McMullan G, Marchant R, Nigam P. Remediation of dyes in textile effluent: A critical review on current treatment technologies with a proposed alternative. Bioresour Technol. 2001;77:247–255.
10. Aksu Z. Application of biosorption for the removal of organic pollutants: A review, process Biochem. 2005;40:997–1026.
11. Han R, Zou W, Yu W, Yuanfeng CW, Shi J. Biosorption of methylene blue from aqueous solution by fallen phoenix tree's leaves. J Hazard Mater. 2001;141:56–162.
12. Nasuha N, Hameed BH, Mohd Din AT. Rejected tea as a potential low-cost adsorbent for the removal of methylene blue. J Hazard Mater. 2010;175:126–132.
13. Han R, Wang Y, Yu W, Zou W, Shi J, Liu H. Biosorption of methylene blue from aqueous solution by rice husk in a fixed-bed column. J Hazard Mater. 2007;141:713–718.
14. Zhou Q, Gong W, Yang D, Xie C, Li Y, Liu X, et al. Assessment of the biosorption characteristics of a spent cottonseed husk substrate for the decolorization of methylene blue. Clean – Soil, Air, Water. 2011;39(12):1087–1094.
15. Nac'era Y, Aicha B. Equilibrium and kinetic modelling of methylene blue biosorption by pretreated dead *Streptomyces rimosus*: Effect of temperature. Chem Eng J. 2006;119:121–125
16. Han RP, Wang YF, Han P, Shi J, YangJ, Lu YS. Removal of methylene blue from aqueous solution by chaff in batch mode. J Hazard Mater. 2006;B137:550-557.
17. Otero M, Rozada F, Calvo LF, Garcia AI, Mor'an A. Kinetic and equilibrium modelling of the methylene blue removal from solution by adsorbent materials produced from sewage sludges. Biochem Eng J. 2003;15:59–68.
18. Garg VK, Amita M, Kumar R, Gupta R. Basic dye (methylene blue) removal from simulated wastewater by adsorption using Indian rosewood sawdust: A timber industry waste. Dyes Pigments. 2004;63:243–250.
19. Waranusantigula P, Pokethitiyooka P, Kruatrachuea M, Upatham ES. Kinetics of basic dye (methylene blue) biosorption by giant duckweed (*Spirodela polyrrhiza*),” Environ Pollution. 2003;125:385–392.
20. Fuchs E. Keratins and the Skin. Ann. Rev. cell Dev. Biology. 1995;111:23-153.
21. BBC News. The unusual uses for animal body parts; June 2011. Available: www.bbc.co.uk/news/mobile/science-environment-13670184.
22. Arica MY, Bayramoglu G. Biosorption of Reactive Red 120 dye from aqueous solution by native and modified fungus biomass preparations of *Lentinus sajorcaju*, J Hazard Mater. 2007;149:499–507.
23. Donald LP, Gary ML, George SK. Introduction to spectroscopy: A guide for students of organic chemistry. 1st ed. Toronto: WB Saunders Company; 1979.
24. Kumara KV, Porkodi K. Mass transfer, kinetics and equilibrium studies for the biosorption of methylene blue using *Paspalum notatum*,” J Hazard Mater. 2007;146: 214–226.

25. Mall ID, Srivastava VC, Kumar GVA, Mishra IM. Characterization and utilization of mesoporous fertilizer plant waste carbon for adsorptive removal of dyes from aqueous solution. *Colloids and Surfaces A Physicochem Eng Aspects*. 2006;278:175–187.
26. Nady AF, Ola IE, Laila BK. Effectiveness of Alkali-Acid Treatment in Enhancement the Adsorption Capacity for Rice Straw: The Removal of Methylene Blue Dye. *ISRN Physical Chem*. 2013;2013:1-15
27. Abdallah R, Taha S. Biosorption of methylene blue from aqueous solution by nonviable *Aspergillus fumigatus*. *Chem Eng J*. 2012;195:69–76.
28. Gupta S, Babu BV. Removal of toxic metal Cr (VI) from aqueous solutions using sawdust as adsorbent: Equilibrium, kinetics and regeneration studies. *Chem Eng*. 2009;150:352–365.
29. Aksu Z, Tezer S. Biosorption of reactive dyes on the green alga *Chlorella vulgaris*. *Process Biochem*. 2005;40:1347–1361.
30. Langmuir I. The adsorption of gases on plane surfaces of glass, mica and platinum. *J Am Chem Soc*. 1918;40:1361–1403.
31. Freundlich HMF. Über die adsorption in lösungen, *Z. Phys. Chem*. 1906;57:385-470.
32. Temkin M. Die gas adsorption und der nernstsche wärmesatz. *Acta Physicochim URSS* 1934;1:36–52.
33. Dubinin MM. The potential theory of adsorption of gases and vapors for adsorbents with energetically non-uniform surface. *Chem Rev*. 1960;60:235–266.
34. Argun ME, Dursun S, Ozdemir C, Karatas M. Heavy metal adsorption by modified oak sawdust: Thermodynamics and kinetics. *J.Hazard Mater*. 2007;141:77–85.
35. Osasona I, Adebayo AO, Ajayi OO. Adsorptive removal of chromium (VI) from aqueous solution using cow hooves. *J Sci Res Reports*. 2013;2(1):288-303.
36. Vadivelan V, Kumar KV, Equilibrium, kinetics, mechanism, and process design for the sorption of methylene blue onto rice husk, *J Colloid Interface Sci*. 2005;286:90–100.
37. Xiong, XJ Meng XJ, Zheng TL. Biosorption of C.I. Direct Blue 199 from aqueous solution by nonviable *Aspergillus niger*, *J Hazard Mater*. 2010;175:241–246.
38. Pavan FA, Lima EC, Dias SLP, Mazzocato AC. Methylene blue biosorption from aqueous solutions by yellow passion fruit waste. *J Hazard Mater*. 2008;150:703–712.
39. Lagergren S. About the theory of so-called adsorption of soluble substance. *Kung Sven Vetén Hand*. 1898;24:1–39.
40. Ho YS, McKay G. Kinetic models for the sorption of dye from aqueous solution by wood. *J Environ Sci Health Part B: Process Saf Environ Prot*. 1998;76:183–191.
41. Weber WJ, Morris JC. Kinetics of adsorption on carbon from solution. *J. Sanitary Eng Div Am Soc Chem Eng*. 1963;89:31–59.

© 2013 Osasona et al.; This is an Open Access article distributed under the terms of the Creative Commons Attribution License (<http://creativecommons.org/licenses/by/3.0>), which permits unrestricted use, distribution, and reproduction in any medium, provided the original work is properly cited.

Peer-review history:

The peer review history for this paper can be accessed here:
<http://www.sciencedomain.org/review-history.php?iid=226&id=5&aid=1631>